Research Article

Alberto Boretti* and Ayman al Maaitah

Dispatchable power supply from beam down solar point concentrator coupled to thermal energy storage and a Stirling engine

https://doi.org/10.1515/ehs-2021-0053
Received October 29, 2021; accepted May 22, 2022;
published online June 6, 2022

Abstract: A high concentration high-temperature beam down solar point concentrator is proposed, coupled to thermal energy storage and a Stirling engine to deliver fully dispatchable electricity over 24 h. Full 24 h operation at nominal power is permitted during the month of maximum solar energy collection while in the month of minimum solar energy collection, the full power production is limited to 17.06 h. The monthly average capacity factors oscillate between 71 and 100%, with an average of 87.5%. Thanks to an electric heater for the heat storage fluid, the system can accept excess electricity from the grid to compensate for the loss of the solar energy collected every other month versus the solar energy collected during the best summer month, to operate at rated power 24 h a day in every day of the year. In this case, the capacity factor can reach 100% every month. By further increasing the size of the thermal energy storage and the power of the engine, the electric thermal energy storage capability of the system can be enhanced, increasing the amount of electricity otherwise wasted that could be collected from the grid to be then returned when needed.

Keywords: concentrated solar power; higher concentration solar; higher temperature cycles; higher temperature fluids; molten salts; thermal energy storage.

Introduction

Prices for solar photovoltaic and wind renewable energies have arguably reached all-time lows, leading to significantly huge amounts of gigawatts worth of new renewable energy generation, and often to energy surpluses beyond the grid system capacity, that need to be stored for future use. Firming up renewables to ensure that there is always dispatchable energy on demand, no matter the time of day or weather, is one of the biggest challenges in the power generation, transmission, and distribution industries and utilities. We must have a way to store renewable energy for later use. A grid feed by solar photovoltaic and/or wind renewable energy sources poses a great challenge because of the inherent intermittency and unpredictability of the sources. This necessitates the use of the unaffordable huge battery energy storage to make a stable grid (Boretti 2019a, 2019b, 2019c, 2019d, 2019e).

Battery energy storage (BES) has unaffordable environmental and economic costs, and is only suitable for storing a small amount of energy for short periods, but has large round trip efficiency and fast response (Boretti 2021b). Internal thermal energy storage systems are an avenue to deliver a much better-levelised cost of dispatchable electricity (Boretti 2021c). Electric thermal energy storage (eTES) systems are emerging as alternatives to external energy storage to work with large amounts of energy stored over long times, despite suffering from low round trip efficiencies (Enescu et al. 2020).

Concentrated solar power (CSP) with thermal energy storage (TES) have the added value of dispatchability (Forrester 2014; Mehos et al. 2015). Here we consider the option to design a small CSP with TES in the 15–30 KW range to cover the 24 h demand of a microgrid. While this system replaces the solar photovoltaic energy supply, there is the opportunity to integrate this system with the cheaper intermittent power by solar photovoltaic, with different opportunities depending on the relative size of solar photovoltaic, solar concentrator, thermal energy storage, and Stirling engine.

With solar photovoltaic and solar concentrator power systems about the same net power output, the grid may be fed by solar photovoltaic energy during the day, and the energy from the solar concentrator, thermal energy

***Corresponding author: Alberto Boretti**, Johnsonville Road, Johnsonville, Wellington 6037, New Zealand,
E-mail: a.a.boretti@gmail.com. https://orcid.org/0000-0002-3374-0238
Ayman al Maaitah, Wahaj Investment L.L.C., Dubai, UAE,
E-mail: Ayman@wahajsolar.com

storage, and Stirling engine during the night. In this case, the size of the TES and the Stirling engine is doubled versus the standalone system, for the same energy supply over a day.

With the solar photovoltaic system largely exceeding the solar concentrator power system net power output, the grid may be fed by solar photovoltaic energy during the day, with extra energy used to warm up the molten salts in the thermal energy storage, and the energy from the solar concentrator and the recycled solar photovoltaic, thermal energy storage and Stirling engine during the night. In this case, an electric heater must be added between the cold and hot tanks of the storage.

The latest CSP research and development activities steer towards higher temperatures in the solar tower (ST) plants with TES (Mehos et al. 2017). This is targeted by the use of novel heat transfer/thermal heat storage fluids and higher efficiency power cycles, such as supercritical CO_2 (sCO_2) (Ahn et al. 2015; Crespi et al. 2017; Mehos et al. 2017; Neises and Turchi 2014; Wright et al. 2010; Zhu 2017), or advanced ultra-supercritical (AUSC) steam Rankine cycles (GEa; GEb; GEc; Kowalczyk et al. 2016; Nicol 2013; Tanuma 2017; Tominaga 2017; Weitzel 2011). AUSC cycles are available for temperatures up to 730 °C. They have an excellent technology readiness level (TRL). sCO_2 has been proposed for even higher temperatures, above 800 °C, but have a lower TRL. Both solutions may deliver thermal efficiencies above 50% but are impractical for small sizes. Off-the-shelf microturbines are not very sophisticated and have typically thermal efficiencies of about 20%. This is the reason why we use a Stirling engine.

High temperatures are only achieved in point solar concentrators, such as parabolic dishes or solar towers surrounded by a field of heliostats. Only the parabolic dish is of interest for small installations. The parabolic dish can reach very high concentration ratios and optical efficiency theoretically almost 100%. However, there are disadvantages. The focal point is moving in space. Transport of the heat transfer/storage fluid (HTF/HSF) from/to the TES is difficult. The solid cross-sectional area of the parabolic dish results in a high wind load on its structure. In recent times, Al-Maaitah (Al-Maaitah 2017, 2019) developed a high flux solar concentrator with a lower focal point fixed to the ground and made up of conical reflective rings. A 10 m in diameter concentrator was built and tested in Masdar Institute Solar Platform in Abu Dhabi (UAE). Temperatures above 1000 °C were reached at the fixed focal point even at low DNI (Al-Maaita 2020). Spherical or cylindrical receivers are used to heat HTF to the levels needed for the TES and the downstream use. This concentrator is called ASC (Ayman Solar Concentrator). Like the parabolic dish, the theoretical optical efficiency is 100%. In practice, values of efficiencies up to 91% are delivered. As the wind flows through its conical rings, the wind load is 10% of the parabolic dish of the same dimensions. ASC of 15 or 25 m is possible. The system is modular, as more units can be coupled to feed a single TES with a single power block downstream.

The selection of HTF/HSF and materials is not trivial. Current salt nitrates such as $NaNO_3$–KNO_3 ($NaNO_3$60%–$kNO_3$40%) are limited 620 °C (Crespi et al. 2020; D'Aguanno et al. 2018). Alternatives are FLiNaK (LiF46.5%-NaF11.5%-KF 42%) (International Atomic Energy Agency 2013; Serrano-López, Fradera, and Cuesta-López 2013), MgCl2-KCl (37.5% $MgCl_2$–62.5% KCl) (Crespi et al. 2020; Xu et al. 2018), liquid sodium (Fink and Leibowitz 1995; Heinzel et al. 2017; Li et al. 2017), or Lead-Bismuth Eutectic LBE (Heinzel et al. 2017). $NaNO_3$-KNO_3 use is limited from 220 to 600 °C and costs \$0.8/kg. FLiNaK is limited to 454–1570 °C and costs \$8.6/kg. $MgCl_2$–KCl use is limited to 426–1412 °C and costs only \$0.35/kg. Materials are potentially more demanding with both FLiNaK and $MgCl_2$–KCl for corrosion. Higher temperatures are also challenging. FliNaK has a much higher than $MgCl_2$–KCl product of $\rho{\cdot}c_p$, relevant to the storage. FliNaK and $MgCl_2$–KCl are the presently selected candidates. $MgCl_2$–KCl can be used in between 426 and 1412 °C. Within this range of temperatures, c_p varies between 0.989 and 1.092 kJ kg^{-1} K^{-1}, ρ in between 1668.5 and 1124.3 kg m^{-3}, μ in between 5.73×10^{-3} and 8.57×10^{-3} Pa s, λ in between 0.46 and 0.36 Wm^{-1} K^{-1} and h in between 421,391 and 1,542,352 J kg^{-1} $\rho{\cdot}c_p$ varies between 1650.5 and 1228.1 $\rho{\cdot}c_p$ kJ m^{-3} K^{-1} (Peng 2019). Quality of fluid is relevant and metallurgical challenges in the high temperature high corrosive environment are still demanding despite the significant work that has already been done (Ding et al. 2018; Fernández and Cabeza 2020a, 2020b, 2020c; Kurley et al. 2019; Polimeni et al. 2018; Vidal and Klammer 2019; Wu et al. 2019).

For small plants, such as the ASC installation, Stirling engines may work better than any other alternative. AUSC Steam Rankine cycles or sCO_2 cycles are not supposed to be used for small installations. Additionally, they do not work at very high temperatures.

α-Stirling engines are perfect for small power installations (15–30 KW). Boretti (2021a) presents a model of an α-Stirling engine delivering energy conversion efficiencies of 42% with hydrogen as working fluid and adopting one hot cylinder, one cold cylinder, and one regenerator, with the hot fluid temperature of 800 °C. This efficiency is much higher than current microturbines

working with air, delivering efficiencies of about 20% working at much lower temperatures.

Stirling engines (Kongtragool and Wongwises 2003; Thombare and Verma 2008) have been used for prototype dish Stirling plants reaching energy conversion efficiencies in the mid to high 20% (26–29%). Mahle (Simmonds et al. 2012; Vávra, Červenka, and Takáts 2013) obtained an efficiency above 40% that is well above the 32% mentioned in Singh and Kumar (2018) as the maximum efficiency in current dish Stirling engines. About the same values were computed in Boretti (2021a). While the Stirling engine has not been popular so far for multiple reasons, there are potentials for achieving higher efficiencies through improved design.

Figure 1 presents a scheme of the ASC plus TES plus power cycle by the Stirling engine.

ASC with TES may deliver solar heat continuously at temperatures up to 1100 °C. Synergies of power generation are possible with thermochemical hydrogen production by the same system. The upstream section of solar energy collection and storage is unaltered. The downstream section is specialized for electricity production, hydrogen production, or other high-temperature thermal processes.

Materials and methods

Simulations have been performed by using the National Renewable Energy Laboratory (NREL) System Advisor Model (SAM) (sam.nrel.gov/) for the selected location of Tabuk, Saudi Arabia. The version used is 2020.2.29, now a legacy version of SAM, because the latest versions do not include anymore the dish Stirling model. The weather file for Tabuk, Saudi Arabia has been downloaded from (climate.onebuilding.org) (SAU_TB_Tabuk.403750_TMYx.2004-2018.epw). The baseline ASC 10 m without TES running a Stirling engine is modeled as an equivalent dish-Stirling. The model is fully described in Fraser (2008). The equivalent projected mirror area is 78.5 m^2. The reflectance is 94%. The receiver has an aperture diameter of 0.184 m, insulation of thickness 0.075 m, thermal conductivity 0.06 W m^{-1} K^{-1}, absorber absorptance 0.9, absorber surface area 0.6 m^2, cavity absorptance 0.6, cavity surface area 0.6 m^2, the internal diameter of cavity perp. To aperture 0.46 m^2, internal depth of cavity perp. To aperture 0.46 m^2. The Stirling engine model is based on the Beale curve-fit equation with temperature correction. The coefficients for the Beale curve-fit equation describe the engine's power output as a function of its input power and the engine pressure (Fraser 2008). Peak efficiency (power output to power input) is set to 42%. The nominal electrical power output of the engine-generator set is 25 kW. The Heater Head Set temperature is 1093 K, the Heater Head Lowest Temperature is 1073 K, the engine speed is 1500 rpm, the displaced volume of the engine is 0.00038 m^3.

Results

Preliminary figures

In the Tabuk region (28.401254°, 036.567049°, Tabuk, Tabuk Region, Saudi Arabia), from (globalsolaratlas.info/), the direct normal irradiation (DNI) is 2698.0 kWh m^{-2}, the Global horizontal irradiation (GHI) is 2330.7 kWh/m^2, the Diffuse horizontal irradiation (DIF) is 600.2 kWh m^{-2}, the Global tilted irradiation at an optimum angle (GTI Opta) is 2601.1 kWh m^{-2} and the Optimum tilt of PV modules (OPTA) is 29/180°.

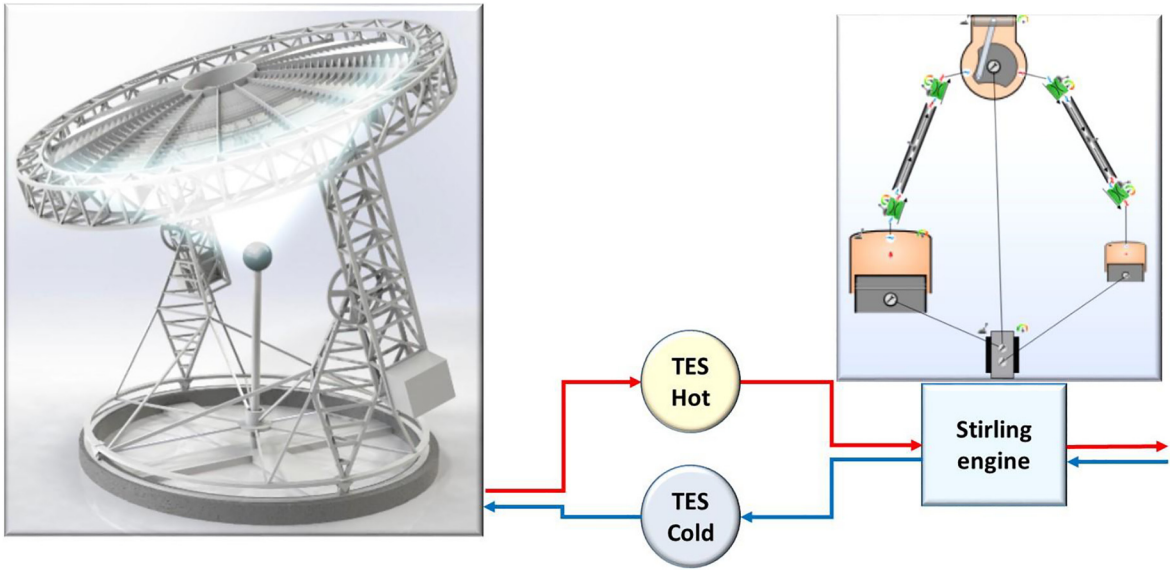

Figure 1: Scheme of the upstream ASC with TES, plus the downstream power cycle represented as the Stirling engine plus the generator.

The design of the TES and the engine are challenging, as maximum and minimum daily solar energies differ considerably because of seasonality and weather. By assuming as first approximation a collector efficiency (collector thermal power produced vs. collector thermal power received) of 88%, and a receiver efficiency inclusive of collector-receiver transmission (receiver thermal power output vs. collector thermal power produced) of 89%, about the same as dishes, totaling 78% of the incident energy, and the only use of the DNI, this translates into thermal energy collected over a year by the 10 m diameter ASC of surface 78.5 m^2 of 166,276 KWh_t per year or 456 KWh_t average per day. Having a power cycle of 32% efficiency as in many off-the-shelf Stirling engine products would translate into production of 53,208 KWh_e per year or 146 KWh_e per day on average. Having a power cycle of 42% efficiency as in the best possible Stirling engines would translate into production of 69,836 KWh_e per year or 191 KWh_e per day on average. In this latter case, the power of the 42% Stirling engine needed to produce electricity 24 h per day would be 8 kW (191 kWh_e/24 h = 7.96 kW) while the TES would have to store 227 kWh_t (191 kWh_e/2/0.42). Obviously, without TES, the power of the engine will have to double to produce the same electricity only during daylight time. Better estimations are possible as soon as the details of the solar input and the power plant are better specified, as discussed in the following section, where the National Renewable Energy Laboratory (NREL) System Advisor Model (SAM) (sam.nrel.gov/) software is used to develop a proper model.

There is also the opportunity of coupling the TES to a solar photovoltaic (PV) system. In this case, the Stirling engine could produce electricity for 12 h during the night by using the thermal energy collected by the CSP and the excess electricity produced by the PV converted to heat. Then, the PV system could produce electricity during the day, also above the demand, with the excess energy stored in the TES.

Following a similar principle to the Azelio "thermal battery", the extra energy from the solar PV systems can be stored in the TES. Despite the round trip efficiency of electric-to-thermal-to-mechanical-to-electric passing through an electric resistance of the Stirling engine and generator being much less than the efficiency of storing and releasing electricity into a lithium-ion battery, this solution has other merits. No lithium-ion battery is needed, and the energy to convert and reuse is only the excess energy. There is the possibility to increase the volume of the TES and use the extra electricity from the PV system to warm up the heat storage fluid through an electric resistance in a separate circuit from the cold to the hot tank. This opportunity only adds the cost of the electric resistance, that however may be needed to ensure the heat transfer fluid does not solidify during extremely cold conditions also in the baseline design, and the enlarged cold and hot volumes and mass for the heat storage fluid. Additional costs for the increased size of pumps, Stirling engine, and electric generator may only follow the specification of the PV plant to be coupled to the CSP with TES and Stirling being considered.

Opposite to the solar PV system that without a battery has production following availability of the resource (apart from tilting and curtailment), the TES of the proposed system permits full dispatchability.

Waste heat (coolant) from the Stirling engine may also be used for applications such as heating or cooling (chiller, hot water). This increases the total efficiency.

To compensate for extreme weather events during the winter, the backup system when the solar radiation is absent for a few days can be a simple burner to generate heat that either power the Stirling engine or add thermal energy to the TES.

NREL SAM simulations

The baseline configuration is no TES and 25 kW Stirling engine of efficiency 42%.

Figure 2 presents in (a)

- collector thermal power input,
- collector thermal power produced/receiver thermal power input,
- receiver thermal power output,

and in (b)

- engine power output

Figure 3 presents in (a)

- monthly energy to engine,

in (b)

- monthly average daily energy to the engine.

Figure 4 finally presents the engine power, the monthly average, min, max, average daily min, and average daily max.

It is to be noted (Figure 4) as the maximum average monthly power of the engine is only 8 kW, despite the maximum being 25 kW. The annual average capacity factor (ratio of the average power of generating electricity to nominal power) is 28%. Additionally, electricity is produced only phased with the resource availability (Figure 2), on average 12 h per day.

From Figures 3 and 4, it is clear that adding 270 kWh of thermal energy storage would permit the operation of a Stirling engine of power reduced to 8 kW over 24 h during the month of maximum solar energy collection (June). In the month of minimum solar energy collection (February), the full power production will be limited to 17.06 h.

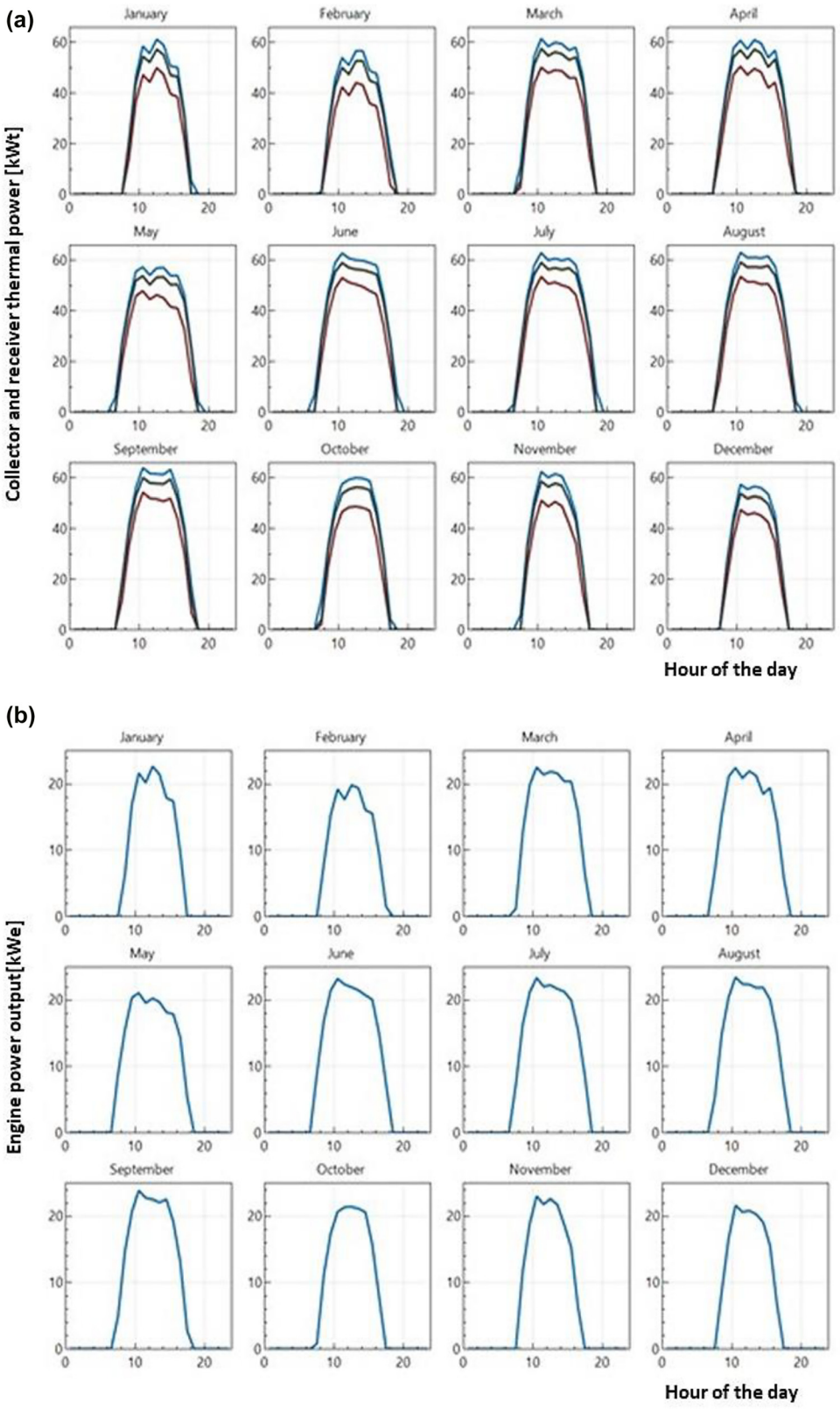

Figure 2: Model results.
(a) Collector thermal power input, collector thermal power produced/receiver thermal power input, and receiver thermal power output [kWt].
(b) Engine power output [kWe]. No TES, Stirling engine power 25 kW.

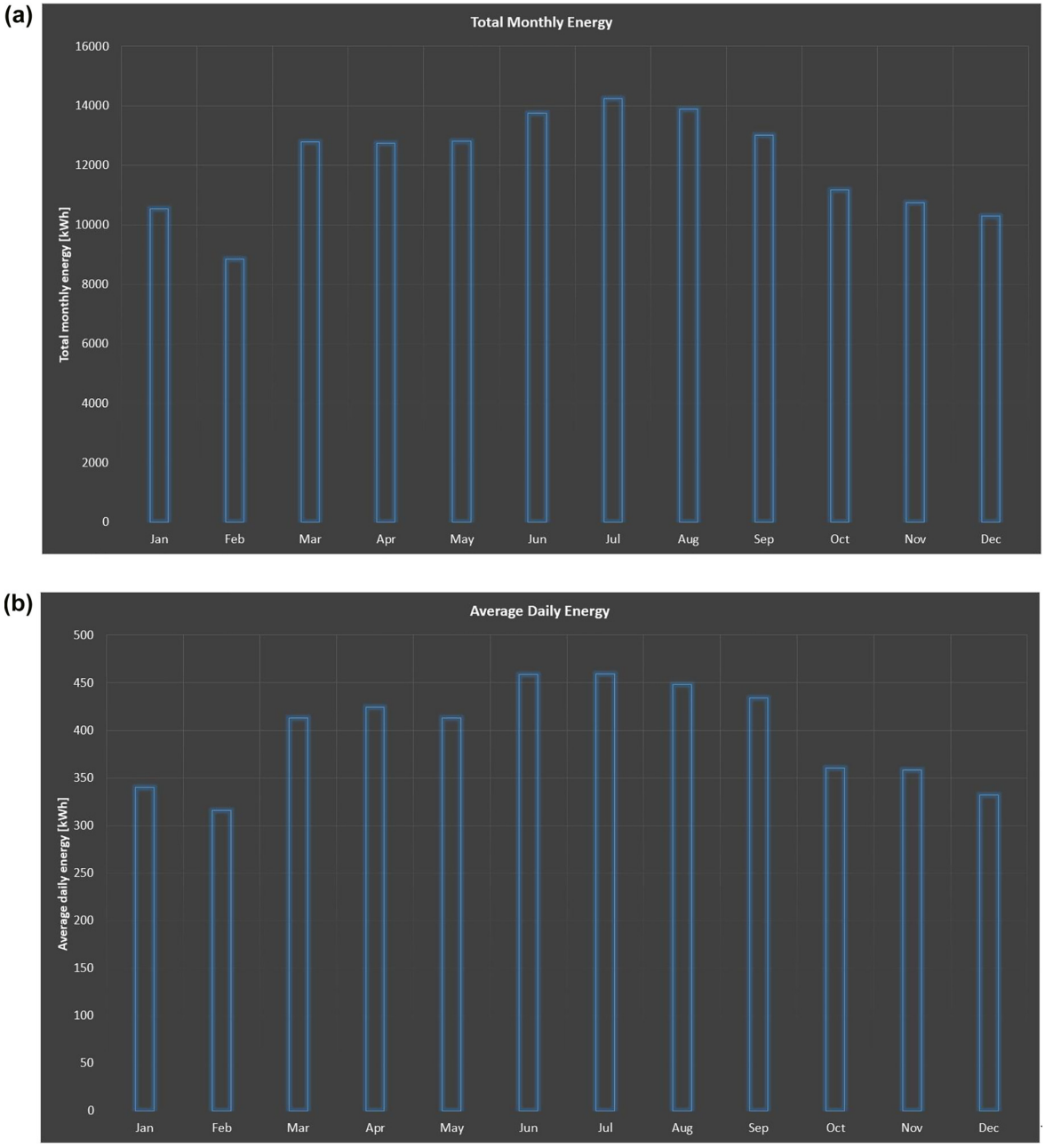

Figure 3: Model results.
(a) Monthly energy to engine [kWh]. (b) Monthly average daily energy to the engine [kWh].

Intermediate results will be obtained in the intermediate months. With this choice, the monthly average capacity factors will oscillate between 71 and 100%, with an average of 87.5%. This is three times the value computed for the case without TES. The Stirling engine is also three times smaller. Figure 5 presents the engine power, the monthly average, min, max, and average daily min and average daily max, in the design with 270 kWh_t of TES and Stirling engine of 8 kW of power.

Further optimizations are possible. The size of the engine and thermal energy storage may be changed to satisfy different load demands, and definitively to store excess electricity from solar photovoltaic in the case of coupling.

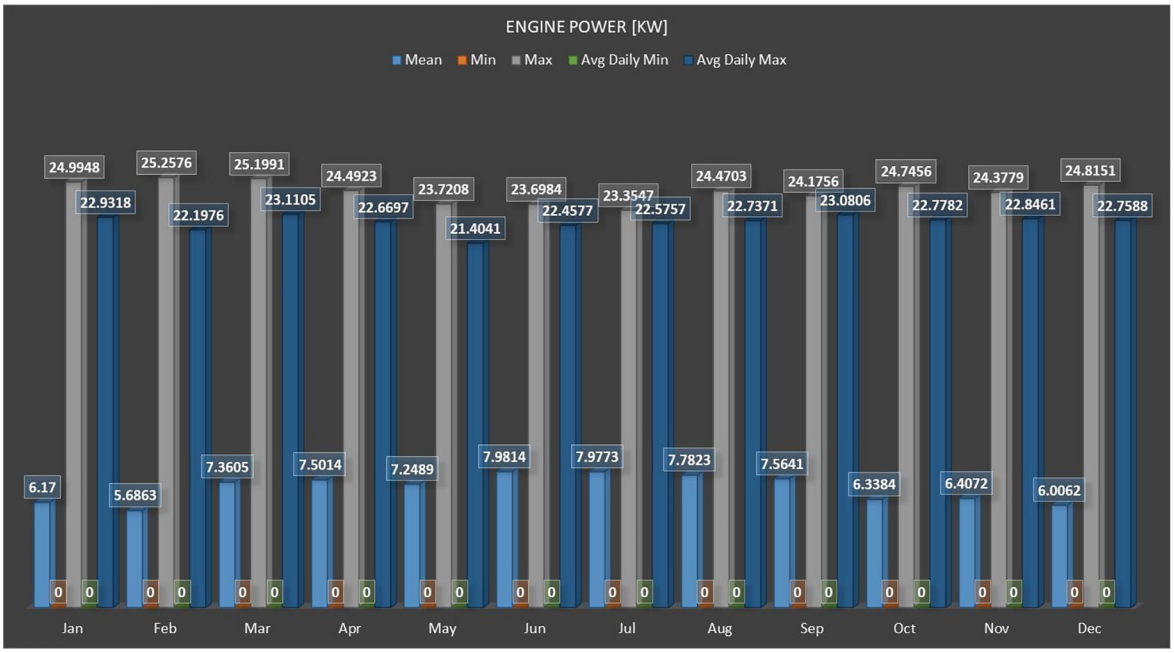

Figure 4: Engine power [kW]. Monthly average, min, max, and average daily min and average daily max. No TES, 25 kW Stirling engine.

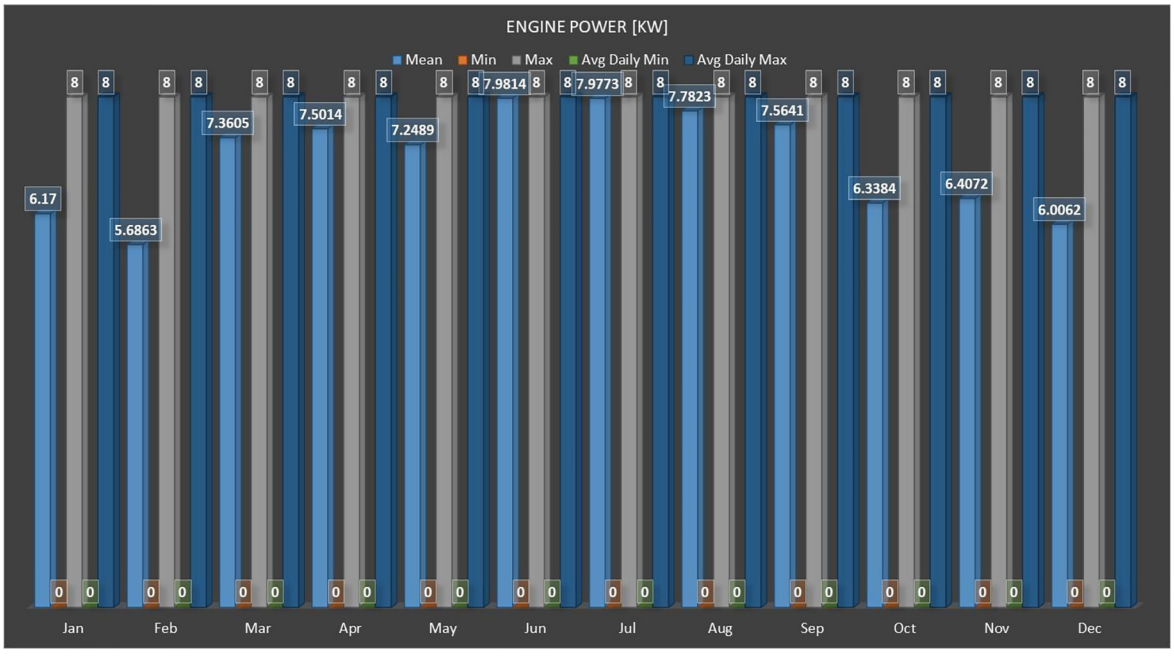

Figure 5: Engine power [kW]. Monthly average, min, max, and average daily min and average daily max. 270 kWh_t TES, 8 kW Stirling engine.

Conclusions

We have proposed a CSP (10 m ASC) with TES (270 kWh) to produce electricity continuously over 24 h at a power of 8 kW through a Stirling engine of efficiency 42%. Full 24 h operation is permitted during the month of maximum solar energy collection while in the month of minimum solar energy collection, the full power production is limited to 17.06 h, and intermediate results are obtained in the intermediate months. The monthly average capacity factors

oscillate between 71 and 100%, with an average of 87.5%. By collecting excess electricity from the grid moving apart from the month of maximum solar energy collection, warming up the heat storage fluid through an electric resistance, this electricity can be stored and released at no extra cost, with a round trip efficiency approaching 42% efficiency of the Stirling engine multiplied by the efficiency of the electric heater. In this case, the operation may be guaranteed for 24 h all the year, and capacity factors can be always 100% (excluding maintenance, failures, and exceptional circumstances). This use of the electric heater, TES, and Stirling engine comes at practically no cost but is limited every month to the amount of solar energy in defect of the best summer month solar energy. It is possible to further expand the electric thermal energy storage capability by simply enlarging the TES system and adopting a more powerful Stirling engine, to accept extra excess electricity from the grid to be stored and released with round trip efficiencies approaching the 42% of the Stirling cycle.

Author contributions: AB: conceptualization. AB, and AA-M: writing—original draft preparation and writing—review and editing. AA-M and AB: visualization. All authors have read and agreed to the published version of the manuscript.
Research funding: None declared.
Conflict of interest statement: AA-M is one of the owners of the company Wahaj Investment L.L.C. The other author declares that the research was conducted in the absence of any commercial or financial relationships that could be construed as a potential conflict of interest.

References

Ahn, Y., S. J. Bae, M. Kim, S. K. Cho, S. Baik, J. I. Lee, and J. E. Cha. 2015. "Review of Supercritical CO_2 Power Cycle Technology and Current Status of Research and Development." *Nuclear Engineering and Technology* 47 (6): 647–61.

Al-Maaitah, A. A. 26 September 2017. "Method and Apparatus for Tracking and Concentrating Electromagnetic Waves Coming from a Moving Source to a Fixed Focal Point." U.S. Patent No. 9,772,121 B1.

Al-Maaitah, A. A. 8 October 2019. "System for Collecting Radiant Energy with a Non-imaging Solar Concentrator." U.S. Patent No. US 10,436,182 B2.

Al-Maaita, A. A. 2020. "Design & Demonstration of a 10-Meter Metallic Reflector-Based Fresnel Lens, with Lower Focal Point Fixed to the Ground." In *Proceedings of the 26th SolarPACES conference*, Sept. 28–October 2nd, 2020. cms2020. Also available at solarpaces-conference.org/file/display_attachment/ab37be5b91c0133a162b848b87bcc27?filename=Ayman+Al-Maaitah+-+Paper.pdf.

Boretti, A. 2019a. "Energy Storage Requirements to Address Wind Energy Variability." *Energy Storage* 1 (5): e77.

Boretti, A. 2019b. "Energy Storage Needs for an Australian National Electricity Market Grid Without Combustion Fuels." *Energy Storage*, https://doi.org/10.1002/est2.92.

Boretti, A. 2019c. "Dependent Performance of South Australian Wind Energy Facilities with Respect to Resource and Grid Availability." *Energy Storage* 1 (6): e97.

Boretti, A. 2019d. "High-Frequency Standard Deviation of the Capacity Factor of Renewable Energy Facilities – Part 1: Solar Photovoltaic." *Energy Storage*, https://doi.org/10.1002/est2.101.

Boretti, A. 2019e. "High-Frequency Standard Deviation of the Capacity Factor of Renewable Energy Facilities – Part 2: Wind." *Energy Storage* 1 (6): e100.

Boretti, A. 2021a. "α-Stirling Hydrogen Engines for Concentrated Solar Power." *International Journal of Hydrogen Energy* 46 (29): 16241–16247.

Boretti, A. 2021b. "Solar Photovoltaic and Batteries Have Unaffordable Environmental and Economic Costs." *Energy Storage* 3 (3): e206.

Boretti, A. 2021c. "Integration of Solar Thermal and Photovoltaic, Wind, and Battery Energy Storage through AI in NEOM City." *Energy and AI* 3: 100038.

Crespi, F., G. Gavagnin, D. Sánchez, and G. S. Martínez. 2017. "Supercritical Carbon Dioxide Cycles for Power Generation: A Review." *Applied Energy* 195: 152–83.

Crespi, F., D. Sánchez, G. S. Martínez, T. Sánchez-Lencero, and F. Jiménez-Espadafor. 2020. "Potential of Supercritical Carbon Dioxide Power Cycles to Reduce the Levelised Cost of Electricity of Contemporary Concentrated Solar Power Plants." *Applied Sciences* 10 (15): 5049.

climate.onebuilding.org.

D'Aguanno, B., M. Karthik, A. N. Grace, and A. Floris. 2018. "Thermostatic Properties of Nitrate Molten Salts and Their Solar and Eutectic Mixtures." *Scientific Reports* 8 (1): 1–15.

Ding, W., A. Bonk, and T. Bauer. 2018. "Corrosion Behavior of Metallic Alloys in Molten Chloride Salts for Thermal Energy Storage in Concentrated Solar Power Plants: A Review." *Frontiers of Chemical Science and Engineering* 12 (4): 564–76.

Enescu, D., G. Chicco, R. Porumb, and G. Seritan. 2020. "Thermal Energy Storage for Grid Applications: Current Status and Emerging Trends." *Energies* 13 (2): 340.

Forrester, J. 2014. "The Value of CSP with Thermal Energy Storage in Providing Grid Stability." *Energy Procedia* 49: 1632–41.

Fink, J. K., and L. Leibowitz. 1995. *Thermodynamic and Transport Properties of Sodium Liquid and Vapor (No. ANL–RE-95/2)*. Argonne National Lab.

Fernández, A. G., and L. F. Cabeza. 2020. "Corrosion Evaluation of Eutectic Chloride Molten Salt for New Generation of CSP Plants. Part 1: Thermal Treatment Assessment." *Journal of Energy Storage* 27: 101125.

Fernández, A. G., and L. F. Cabeza. 2020. "Corrosion Evaluation of Eutectic Chloride Molten Salt for New Generation of CSP Plants. Part 2: Materials Screening Performance." *Journal of Energy Storage* 29: 101381.

Fernández, A. G., and L. F. Cabeza. 2020. "Cathodic Protection Using Aluminum Metal in Chloride Molten Salts as Thermal Energy Storage Material in Concentrating Solar Power Plants." *Applied Sciences* 10 (11): 3724.

Fraser, P. R. 2008. *Stirling Dish System Performance Prediction Model*. University of Wisconsin Master Thesis. Also available at sel.me.wisc.edu/publications/theses/fraser08.zip.

GE. *Ultra-Supercritical & Advanced Ultra-Supercritical Technology*. Also available at www.ge.com/power/steam/steam-power-plants/advanced-ultra-supercritical-usc-ausc.

GE. *Steam Power Product Catalog*. Also available at www.ge.com/content/dam/gepower-steam/global/en_US/documents/Steam-Product-Catalog.pdf.

GE. *GE's STF-D Series Reheat Steam Turbines*. Also available at www.ge.com/power/steam/steam-turbines/reheat.

http://globalsolaratlas.info/.

Heinzel, A., W. Hering, J. Konys, L. Marocco, K. Litfin, G. Müller, J. Pacio, C. Schroer, R. Stieglitz, L. Stoppel, and A. Weisenburger. 2017. "Liquid Metals as Efficient High-Temperature Heat-Transport Fluids." *Energy Technology* 5 (7): 1026–36.

International Atomic Energy Agency. 2013. *Challenges Related to the Use of Liquid Metal and Molten Salt Coolants in Advanced Reactors*. IAEA-TECDOC-1696.

Kowalczyk, Ł., W. Elsner, P. Niegodajew, and M. Marek. 2016. "Gradient-free Methods Applied to Optimisation of Advanced Ultra-supercritical Power Plant." *Applied Thermal Engineering* 96: 200–8.

Kurley, J. M., P. W. Halstenberg, A. McAlister, S. Raiman, S. Dai, and R. T. Mayes. 2019. "Enabling Chloride Salts for Thermal Energy Storage: Implications of Salt Purity." *RSC advances* 9 (44): 25602–8.

Kongtragool, B., and S. Wongwises. 2003. "A Review of Solar-Powered Stirling Engines and Low-Temperature Differential Stirling Engines." *Renewable and Sustainable Energy Review* 7 (2): 131–54.

Li, H., X. Zhang, Y. Sun, and M. Li. 2017. "Thermodynamic Properties of Liquid Sodium under High Pressure." *AIP Advances* 7 (4): 045305.

Mehos, M., J. Jorgenson, P. Denholm, and C. Turchi. 2015. "An Assessment of the Net Value of CSP Systems Integrated with Thermal Energy Storage." *Energy Procedia* 69: 2060–71.

Mehos, M., C. Turchi, J. Vidal, M. Wagner, Z. Ma, C. Ho, W. Kolb, C. Andraka, and A. Kruizenga. 2017. *Concentrating Solar Power Gen3 Demonstration Roadmap (No. NREL/TP-5500-67464)*. Golden, CO (United States): National Renewable Energy Lab.(NREL).

Neises, T., and C. Turchi. 2014. "A Comparison of Supercritical Carbon Dioxide Power Cycle Configurations with an Emphasis on CSP Applications." *Energy Procedia* 49: 1187–96.

Nicol, K. 2013. *Status of Advanced Ultra-supercritical Pulverised Coal Technology*. London: IEA Clean Coal Centre.

Peng, Y. 2019. *High-Temperature Corrosion Study of Alloys in Molten MgCl2-KCl Eutectic Salt*. Tuscaloosa: The University of Alabama.

Polimeni, S., M. Binotti, L. Moretti, and G. Manzolini. 2018. "Comparison of Sodium and KCl-$MgCl_2$ as Heat Transfer Fluids in CSP Solar Tower with sCO_2 Power Cycles." *Solar Energy* 162: 510–24.

Serrano-López, R., J. Fradera, and S. Cuesta-López. 2013. "Molten Salts Database for Energy Applications." *Chemical Engineering and Processing: Process Intensification* 73: 87–102.

Simmonds, S., R. Corbishley, J. Hughes, G. Teylor, H. Hoffmann, P. Wieske, I. Reynols, and D. Wise. 2012. "The Development of the MAHLE 25kWe Solar Heated Stirling Engine." In *15th International Stirling Engine Conference*. Also available at www.mahle-powertrain.com/media/mahle-powertrain/news-and-press/conference-papers/2012/mahle_solar_stirling_engine_development__abs_4.pdf.

Singh, U. R., and A. Kumar. 2018. "Review on Solar Stirling Engine: Development and Performance." *Thermal Science and Engineering Progress* 8: 244–56.

http://sam.nrel.gov/.

Tanuma, T., ed. 2017. *Advances in Steam Turbines for Modern Power Plants*. Cambridge: Woodhead Publishing.

Tominaga, J. 2017. "Steam Turbine Cycles and Cycle Design Optimization: Advanced Ultra-supercritical Thermal Power Plants and Nuclear Power Plants." In *Advances in Steam Turbines for Modern Power Plants*, 41–56. Sawston: Woodhead Publishing.

Thombare, D. G., and S. K. Verma. 2008. "Technological Development in the Stirling Cycle Engines." *Renewable and Sustainable Energy Reviews* 12 (1): 1–38.

Vidal, J. C., and N. Klammer. 2019. "July. Molten Chloride Technology Pathway to Meet the US DOE Sunshot Initiative with Gen3 CSP." In *AIP Conference Proceedings*, Vol. 2126, No. 1, p. 080006. AIP Publishing LLC.

Vávra, J., L. Červenka, and M. Takáts. 2013. "Mathematical Model of a Real Stirling Engine Calibrated by Experiments." *Journal of Middle European Construction and Design of Cars* 2: 2–20.

Wright, S. A., R. F. Radel, M. E. Vernon, G. E. Rochau, and P. S. Pickard. 2010. *Operation and Analysis of a Supercritical CO_2 Brayton Cycle*. Sandia Report, No. SAND2010-0171.

Weitzel, P. S. 2011. "Steam Generator for Advanced Ultra Supercritical Power Plants 700C to 760C." In Weitzel, P. S. 2011. "Steam Generator for Advanced Ultra Supercritical Power Plants 700C to 760C." In *ASME Power Conference*, Vol. 44595, 281–91, https://doi.org/10.1115/power2011-55039.

Wu, F., S. Roy, A. S. Ivanov, S. K. Gill, M. Topsakal, E. Dooryhee, M. Abeykoon, G. Kwon, L. C. Gallington, P. Halstenberg, and B. Layne. 2019. "Elucidating Ionic Correlations beyond Simple Charge Alternation in Molten MgCl2–KCl Mixtures." *The journal of physical chemistry letters* 10 (6): 7603–10.

Xu, X., X. Wang, P. Li, Y. Li, Q. Hao, B. Xiao, H. Elsentriecy, and D. Gervasio. 2018. "Experimental Test of Properties of KCl–$MgCl_2$ Eutectic Molten Salt for Heat Transfer and Thermal Storage Fluid in Concentrated Solar Power Systems." *Journal of Solar Energy Engineering* 140: 6.

Zhu, Q. 2017. *Power Generation from Coal Using Supercritical CO_2 Cycle. Tech. Rep. CCC/280*. International Energy Agency (IEA).